TISSUE ENGINEERING: Part A
Volume 20, Numbers 21 and 22, 2014

DOI: 10.1089/ten.tea.2013.0549

Three-Dimensional Extracellular Matrix Scaffolds by Microfluidic Fabrication for Long-Term Spontaneously Contracted Cardiomyocyte Culture

Jeng-Chun Mei, MS,[1] Aden Yuan Kun Wu, BS,[2] Po-Chen Wu, MS,[1] Nai-Chen Cheng, MD, PhD,[2] Wei-Bor Tsai, PhD,[1] and Jiashing Yu, PhD[1]

To repair damaged cardiac tissue, the important principle of *in vitro* cell culture is to mimic the *in vivo* cell growth environment. Thus, micro-sized cells are more suitably cultured in three-dimensional (3D) than in two-dimensional (2D) microenvironments (ex: culture dish). With the matching dimensions of works produced by microfluidic technology, chemical engineering and biochemistry applications have used this technology extensively in cellular works. The 3D scaffolds produced in our investigation has essential properties, such has high mass transfer efficiency, and variable pore sizes, to adapt to various needs of different cell types. In addition to the malleability of these innovative scaffolds, fabrication procedure was effortless and fast. Primary neonatal mice cardiomyocytes were successfully harvested and cultured in 3D scaffolds made of gelatin and collagen. Gelatin and gelatin–collagen scaffold were produced by the formation of microbubbles through a microfluidic device, and the mechanical properties of gelatin scaffold and gelatin–collagen scaffold were measured. Cellular properties in the microbubbles were also monitored. Fluorescence staining results assured that cardiomyocytes could maintain *in vivo* morphology in 3D gelatin scaffold. In addition, it was found that 3D scaffold could prolong the contraction behavior of cardiomyocytes compared with a conventional 2D culture dish. Spontaneously contracted behavior was maintained for the longest (about 1 month) in the 3D gelatin scaffold, about 19 days in the 3D gelatin–collagen scaffold. To sum up, this 3D platform for cell culture has promising potential for myocardial tissue engineering.

Introduction

Due to the lack of organ donors and complications associated with immune suppressive treatments, scientists and surgeons are continuously looking for new strategies to ameliorate symptoms after myocardial infarction.[1–3] For this reason, myocardial tissue engineering is regarded as a promising solution to heart failure problems.[4–6] Recently, various methods to myocardial tissue engineering had been developed, including three-dimensional (3D) printing technology,[7–9] cardiac patches for implantation,[10] direct cell injection,[11,12] and biomaterial-based scaffold.[13–16] By using biomaterial based scaffolds, made of either natural or synthetic polymeric materials as a ''vehicle,'' we can transplant cardiac cells onto the diseased regions of the heart.[17]

A heart is composed of two major types of cells, cardiomyocytes and cardiac fibroblasts.[18] Synchronous contraction of the entire heart is facilitated via conduction of electrochemical signals though inter-cellular connection via connexin pores. A cellular matrix biomimetic system for myocardial tissue is not currently available due to the complexity of heart tissue and the difficulties of culturing cardiomyocytes *in vitro* for prolonged periods of time.[19] Although an improved protocol for primary neonatal mice cardiomyocyte had been published,[20] however, the cost of culture medium was very expensive, due to the additional supplements, and the substrate culturing cells was on traditional two-dimensional (2D) culture dishes, which are neither biocompatible nor biodegradable.[21,22] Recent developments have shown to provide promising results by culturing cardiomyocytes on biomaterial-based substrates.[23–25] However, several essential characteristic of cultured cardiomyocytes such as their state of health, proof of spontaneous contraction ability, and the sustainability of this spontaneous contraction ability were not comprehensive. Therefore, creating a vehicle that is not only biocompatible and biodegradable but also suitable for cardiomyocytes and cardiac fibroblast survival and contraction is an important goal in myocardial tissue engineering.

Many researchers have created cell sheet-based bioengineered myocardial tissues to mimic cardiomyocyte tissue *in vitro*.[26–28] Some studies also recorded cardiomyocyte contraction behavior on various substrates.[29,30] According to

[1]Department of Chemical Engineering, National Taiwan University, Taipei, Taiwan.
[2]College of Medicine, National Taiwan University, Taipei, Taiwan.

the publications mentioned earlier, cardiomyocytes cultured in a 3D microenvironment, which is closer to natural heart tissue, managed to prolonge the properties of cultured cardiomyocytes mentioned earlier, and therefore exhibits promising potential in cardiac tissue engineering.

To fabricate 3D cell culture scaffolds, encapsulation technique[31] and lyophilization[32] were often used. However, in both techniques, mass transport is a big challenge in 3D cell culture; that is, when the diameter of the tissue is larger than 1 mm, the center of the tissue mass would become hypoxic and low in nutrient content and only peripheral cells could survive. Therefore, scaffolds should satisfy several requirements to provide a suitable environment for 3D cell culture. Highly porous scaffolds, with pore diameters greater than the cell diameter, provide space within the scaffold for tissue development and mass transfer while enabling cells from the surrounding tissue to migrate into the scaffold.[33–35] Therefore, porous scaffolds for 3D cell culture can provide a dynamic cell culture environment, facilitating the exchange of oxygen, nutrition, and wastes.

Generally, 3D cell culture scaffolds have the following advantages: First, 3D scaffolds add a third dimension to the cellular environment, which may generate significant differences in cellular behavior and characteristics and create a greater similarity to conditions in a living organism (e.g., human being).[36,37] Second, they mimic the *in vivo* microenvironments for cells under *in vitro* condition. The 3D structure of an organ is essential to its function. Theoretically, 3D cell culture can provide more valuable data for more practical applications. Since cells are micro-sized, using microfluidic techniques for 3D cell culture scaffold production is the current trend.[38,39] For example, Lin and coworkers apply the microfluidic technique to generate micro bubbles, and then fabricate the bubbles into porous scaffolds for 3D cell culturing.[40,41]

In our studies, to construct a physiologically relevant microenvironment, we created extracellular matrix (ECM)-based micro bubbles to mimic the 3D cell culture environment using microfluidics. Type I collagen and gelatin, two of the ECM molecules, were selected as the scaffolding materials for cell seeding. Collagen is the most abundant protein in mammals, especially in the heart, and it was first used for cardiac scaffolds. However, collagen was not the best candidate for the cardiac scaffold, due to its mechanical property or poor structural integrity.[42–44] Gelatin is derived from the collagen inside animal skin and bones. Cells were isolated from neonatal mice. Cells contain two major types, cardiomyocytes and cardiac fibroblasts, and neither can be excluded if we want to obtain healthy myocardial tissue *in vitro*.[45]

The aims of this study were to establish 3D biomaterial-based scaffolds through microfluidics for prolonged cardiomyocyte culture, to maintain not only survivability but also its spontaneous contraction characteristics. Thus, this 3D scaffold should have high mass transfer efficiency, and is biodegradable and biocompatible. For future applications to other cell types, pore size of 3D scaffolds should be tunable, such that different animal cells size could be accommodated. Furthermore, the fabrication method of 3D scaffolds should be effortless and fast. Finally, cytoskeleton distributions, cell morphology, and contraction frequency of cardiomyocytes in both systems (our 3D system vs. culture plate) were examined.

Materials and Methods

Microfluidic device

A planar flow-focusing microfluidic device made of polydimethylsiloxane (Silmore)[41] was used, which comprised two inputs and one output (Fig. 1A). One of the inputs was the liquid flow, and the flow rate was controlled by PhD 2000 syringe pump (Harvard Apparatus). The other one was gas flow, which was adjusted through a pressure gauge (inlet: max 15 kg/cm^2, outlet: 0.5–7 kg/cm^2, 1/4″NPT). Generally, the liquid flow rate ranged from 20 to 80 μL min^{-1} and the air pressure was 5–35 psi. Adjustments of these two parameters would result in different bubble sizes and an air fraction of the final scaffolds. Using microfluidic channels, bubbles were formed on the union of the liquid and gas phase at the orifice (channel width = 15, 30, 60 μm) situated in the middle of the channel (Fig. 1C). Bubbles that were generated were monodispersed, which self-assembled into highly ordered flowing lattices and collected in disc-shaped reservoirs through PE 20 tubing (Lot No. 0307679; Becton Dickinson).

Three-dimensional gelatin scaffold and 3D collagen-doped gelatin scaffold

Gelatin (Lot No. 041M0052V; Sigma) and collagen were used for 3D scaffold fabrication. Both gelatin and collagen

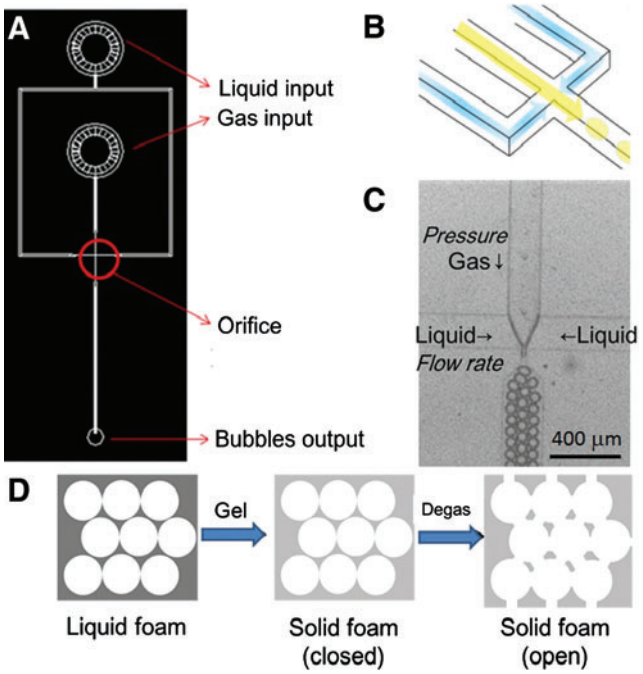

FIG. 1. Bubble formation through microfluidic channels. **(A)** Overall scheme of the microfluidic device, **(B)** three-dimensional (3D) image of the orifice, including liquid section (yellow), gas section (blue), and bubble section (yellow ball), and **(C)** picture of bubble formation under microscope. The gas pressure can be tuned, and the liquid flow rate can be adjusted with a syringe pump. **(D)** The flowchart of scaffold formation. Liquid foam was collected from the microfluidic device and then turned to solid foam by lowering temperature. Finally, the solid foam was put into a vacuum oven to obtain open solid foam, in other words, a 3D scaffold. Color images available online at www.liebertpub.com/tea

were chosen for their abundance (ECM). Gelatin scaffold was fabricated using 7% gelatin and 1% Pluronic® F127 (CAS No. 9003-11-6; Sigma) surfactant solution. Surfactant Pluronic F127 was included to reduce surface tension and has been shown to be biocompatible in cells that proliferate and maintain high viability under 1% concentration.[40] N_2 (FMI) and perfluorohexane (CAS No. 355-42-0; Synquest Laboratories) were used for gas, because perfluorohexane prevented a coarsening phenomenon of bubbles at a longer time. Liquid foam product exiting from the output was collected in a disc-shaped reservoir with 6 mm diameter and 1 mm height. During the process of bubble formation, temperature was maintained above 45°C to keep the solution in liquid form. Bubbles were imaged under a Leica Z16 APO stereomicroscope with an ultrafast camera Miro3 (Vision Research) for 22,000 frames per second. Since gelatin would congeal at a lower temperature, a precooled reservoir was used to contain the end product. After the reservoir was filled, a semi-congealed scaffold was placed in a 4°C refrigerator to solidify the liquid foam quickly. Gelatin was cross-linked by 2% glutaraldehyde (Lot No. MKBD9857; Sigma-Aldrich) in a 4°C refrigerator overnight. It should be noticed that the temperature for storing the liquid foam is not lower than the freezing temperature; this is to avoid the formation of tiny ice crystals inside the gelatin and the creation of microscopic pores which may weaken the mechanical properties of the final scaffolds. According to these procedures, the liquid foam was turned into solid foam (Fig. 1D).

The next day, the solid foam was degased at 7 torr in a vacuum oven (VO-30; HCS) for 2 h. The remaining glutaraldehyde was washed with water, and the solid foam was removed from the reservoir carefully. The solid foam was then soaked in 0.5% sodium borohydride (Aldrich) for 1 h to completely quench autofluorescence. The remaining sodium borohydride was rinsed off with water, and the scaffold was finally degassed again for 2 h. After the degassing step, scaffolds were washed thrice with sterilized phosphate-buffered saline (PBS) and stored in a 1% penicillin/streptomycin/amphotericin solution at 4°C. From these procedures, the solid foams become open solid foams, in other words, 3D scaffolds, for cell culturing (Fig. 1D).

When making collagen-doped gelatin scaffolds, collagen solution was blended with gelatin and Pluronic F127 solution. The concentration of gelatin was maintained at 7%, Pluronic F127 at 1%, and collagen above 1 mg/mL. The procedures for making collagen-doped gelatin scaffolds were similar to those of gelatin scaffold production, except that the scaffolds were placed in PBS solution at 37°C for 1 h for collagen gelation before being stored at 4°C.

Stiffness measurement of 3D porous scaffold

The elastic modulus of the 3D scaffold was determined by self-made equipment with a force sensor (Kyowa) responding to step-by-step compression (Fig. 2B). In each step, the elastic modulus was calculated by dividing the current step strain by a measured stress (Fig. 2A). First, the scaffold was adhered onto the sample well (Fig. 2C); then, the sensor tip was moved to contact the surface of the scaffold; and the current position of the sensor tip was set to be zero strain. A camera was equipped to confirm the sensor

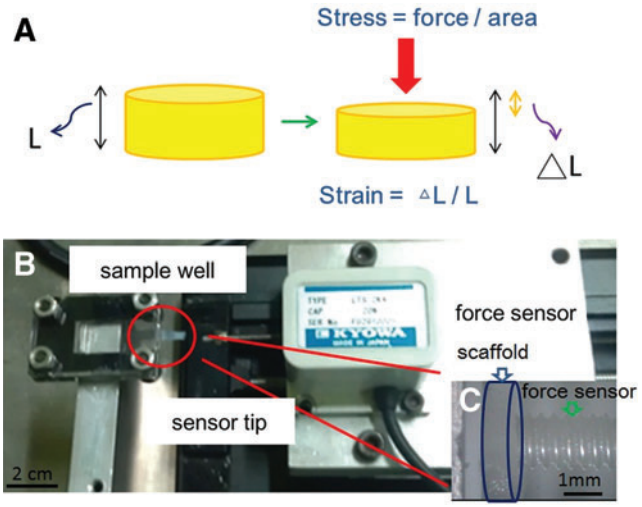

FIG. 2. **(A)** The definition of stress and strain. **(B)** Self-made equipment with a force sensor responding to step-by-step compression. **(C)** Magnification of sample well. A gelatin scaffold was detected by a sensor tip. Color images available online at www.liebertpub.com/tea

tip position. Second, the sensor tip was moved one step long forward to compress the scaffold, while the sensor began recording the force variation at a steady frequency. When the force no longer changed for a period of time, the sensor tip was moved again to further compress the scaffold. The procedure described earlier was repeated until the maximum loading force of the force sensor was reached.

For the 3D scaffold, the total height was 1 mm, and the length of each step was 10 μm; therefore, 1% strain was acquired for each step. The diameter of the scaffold was about 2 mm, and the stress was obtained by dividing the measured force by the surface area. The strain–stress curves and elastic moduli of the 3D scaffolds were obtained.

Cardiomyocyte harvesting and culturing

The investigation was performed in accordance with the Guide for the Care and Use of Laboratory Animals published by the US National Institutes of Health (NIH publication no. 85-23, revised 1996). Primary cardiomyocytes were harvested from neonatal ICR mice (BioLasco Taiwan Co., Ltd.). Briefly, 20 neonatal mice were sacrificed, and the ventricles were taken out. The tissues were first digested at 37°C for 5 min by a digesting enzyme containing 0.1% (w/v) collagenase type II (C6885; Sigma) in HBSS and 0.25% trypsin-EDTA, and the supernatant was discarded. From the second digestion, the supernatant was collected and the reaction was stopped by adding the supernatant to a cold medium that contained fetal bovine serum, penicillin, streptomycin, and amphotericin. The same procedure was repeated 8 to 10 times for collecting cardiomyocytes (also with cardiac fibroblasts), and the cell suspension was passed through a 70 μm mesh. Finally, the cell suspension was seeded onto a gelatin-coated dish for preplating to increase the purity of the cardiomyocytes. The procedure was repeated twice, and the cardiomyocytes in suspension were seeded on a new dish. The number and viability of isolated cardiomyocytes were counted using a hemocytometer with trypan blue

staining. The medium was changed once every 2 days during culturing.

Cell seeding in the scaffold

The scaffold was moved out from the antibiotics solution and soaked in PBS or culture medium for 30 min. A cell suspension with a concentration of about 2×10^6 cells/mL was prepared. Then, the scaffold was placed on filter paper that had been sterilized by UV light. Most of the liquid in the scaffold was sucked by the dry filter paper. After all this, the scaffold became dry and shrunk. With regard to adding cells to the scaffold, cell suspension, in three aliquots of 10 μL, was pipetted on the top of the scaffold. Due to capillarity, the cell suspension was sucked into the scaffold. Furthermore, the cells would be stuck in the porous scaffold, as their size was comparable with the pore size of the 3D scaffold (Fig. 3). The scaffold containing cells was placed in fresh medium, and the medium was changed every 2 days.

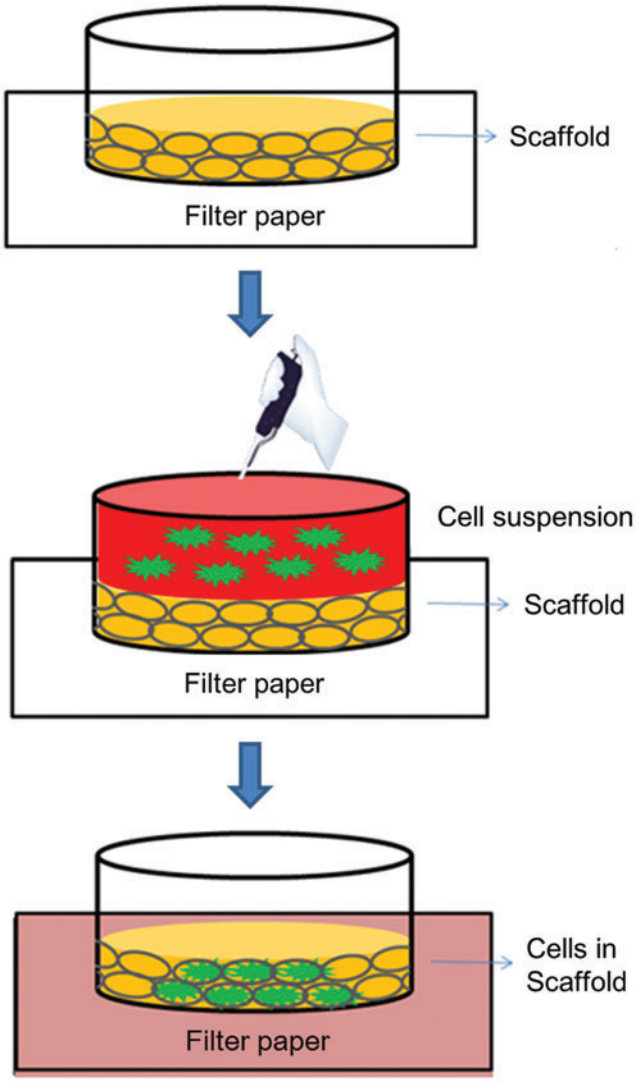

FIG. 3. The flowchart of cell seeding into the 3D scaffold. Color images available online at www.liebertpub.com/tea

Fluorescence staining

For cells cultured in both 2D and 3D environments, the staining protocols[29] were similar. At first, the cell medium was removed, and then PBS was added for rinsing. The cardiomyocytes were fixed with 3.7% paraformaldehyde in cold PBS for 20 min. After fixation, the samples were rinsed by PBS again, followed by permeation with 0.1% Triton X-100 in PBS for 15 min. Blocking against nonspecific binding was performed by incubation in 0.1% PBST containing 2% bovine serum albumin (BSA; Sigma) for 20 min. The samples were then incubated with the primary and secondary antibodies: Monoclonal Anti-α-Actinin (Sarcomeric) antibody produced in mice (ab9465; Abcam) (1:100 dilution in 2% BSA in 0.1% PBST) at room temperature for 1 h followed by Anti-Mouse IgG (whole molecule)–FITC antibody produced in rabbit (F9137, Lot No. 128K4853; Sigma-Aldrich) (1:200 dilution in 2% BSA in 0.1% PBST) at room temperature for 1 h. After the nonbinding antibody was removed from the samples, PBS was used to rinse thrice, for 5 min each. Finally, the nuclei were stained by 100 nM DAPI and the f-actin was stained by 500 nM phalloidin–TRITC. The fluorescence images were acquired by an Inverted Confocal Microscope (LSM 510 META) and NLO DuoScan in the Agricultural Biotechnology Research Center, Academic Sinica, Taiwan. The excitation/emission wavelengths were 405/461 nm for DAPI, 488/518 nm for FITC, and 561/572 nm for phalloidin–TRITC.

Analysis of cell morphology and behavior

Images of the cardiomyocytes cultured both on 2D culture dishes and in 3D scaffolds were taken using a phase-constant microscope at several time points. In addition, the beating behaviors of cardiomyocytes for 2D and 3D cultures were recorded by microscopy and a Charge Coupled Device camera (IMAGINGSOURCE). The cytoskeleton distributions, including f-actin and α-actinin, were investigated and compared using fluorescence staining.

Contraction of cardiomyocytes

The beating frequency is an indication of the health condition of cardiomyocytes.[46] Therefore, the contraction behaviors of cardiomyocytes were recorded under both 2D and 3D culturing. Starting from the 2nd day after the cardiomyocytes were harvested, the spontaneous contractions of cardiomyocytes were recorded by microscopy and a Charge Coupled Device camera, until the cardiomyocytes were no longer contracting. These different results for 2D and 3D cultures were compared and discussed in detail.

Results and Discussion

Morphology of 3D scaffold

The diameter and thickness of the 3D scaffolds were 6 and 1 mm, respectively. Figure 4A shows the scaffolds in closed solid foam state, before being degassed. Finally, we acquired the open solid foam, which not only can accommodate cells, but also is transparent as could be seen under a phase-constant microscope, as shown in Figure 4B. We used the Inverted Confocal Microscope to acquire images of the 3D scaffold at different z-positions; the interval was 1 μm,

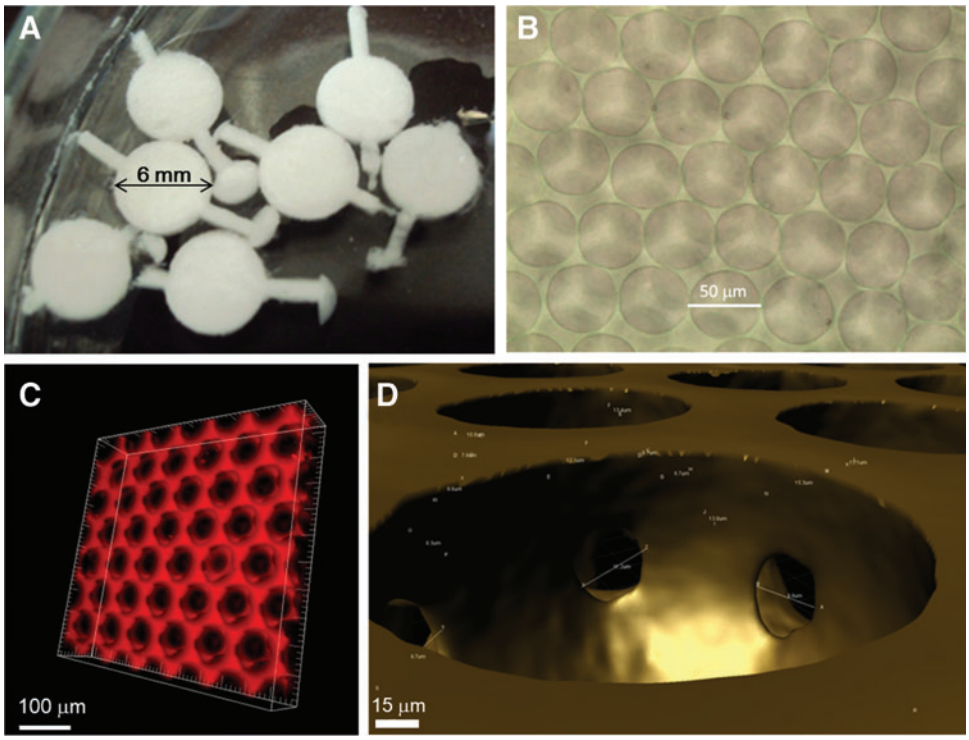

FIG. 4. The morphology of the 3D scaffold. **(A)** The scaffold was just pulled out from the reservoir and was not degassed. **(B)** The scaffold (open solid foam) under a phase-constant microscope. **(C)** 3D scaffold rebuilding by software. **(D)** Interconnecting pores appeared after degassing. Color images available online at www.liebertpub.com/tea

and the total height was 50–100 μm. Then, the series of images were analyzed by painting software to rebuild the morphology of the 3D scaffold, as shown in Figure 4C. The red region indicates the solid structure, whose composition depended on the liquid materials we used, and the black region represents the empty spaces, which accommodated cells for the 3D cell culture. During the degassing, the thinner wall between two bubbles (usually at the position where two bubbles contact each other) broke, because it could not withstand the high pressure difference anymore. We called the broken pores interconnecting pores, which are shown in Figure 4D. The phenomenon kept the culture system interosculated and reduced the resistance of mass transfer; in other words, it increased the gas, nutrition, and waste changing. In addition, the cells in the scaffold lived next to one another and could conduct their chemical and electrical signals to each other through interconnecting pores. Therefore, the cells lived in an open and mass-changeable microenvironment.

Generally, a higher air fraction resulted in a more orderly bubble arrangement in the 3D scaffold. When making scaffolds, we had to ensure that the coarsening time of bubbles was shorter than the gelling time of the materials; otherwise, the scaffolds would collapse during the degassing step. Therefore, the materials in the microfluidic channels should be in liquid form, and the bubbles should turn into solid form as soon as possible after the collection is completed. Although the precooling reservoir increases the resistance of the bubbles going forward, we took advantage of the avoidance of bubble coarsening. Comparing the gelatin scaffold and collagen-doped scaffold, when these two types of hydrogels were dried by filter paper during cell seeding, the latter one retained its original shape, while the former one lost its original shape. Sterilization was very important, because the scaffold was so for cell cultures. Antibiotics were used to suppress the growth of bacteria, and extra attention to the environment was paid in which we carried out the experiments and the materials we used to ensure the scaffolds are not contaminated.

We could easily control the bubble size and air fraction of the final 3D scaffolds using a planar flow-focusing microfluidic device. Regardless of what liquid components we used, as long as the flow rate was increased, both the bubble size and air fraction of 3D scaffolds were decreased. However, if the pressure was increased, both the bubble size and air fraction of 3D scaffolds were increased. Furthermore, the larger the orifice of the microfluidic channel used, the larger the bubble formed, but at a lower operating pressure range. Generally, the bubble size had a positive relationship with the air fraction of scaffolds. In other words, if we want to increase the air fraction, we can increase the bubble size by reducing liquid flow rate or increasing gas pressure.

Stiffnesses of 3D gelatin and collagen-doped gelatin scaffolds

The strain–stress curves (Fig. 5A–C) and the elastic moduli (Table 1) of the culture dish and 3D scaffold were obtained. The strain–stress curves of the culture dish, gelatin scaffold, and gelatin–collagen scaffold are shown in Figure 5A–C, respectively. The reproducibility of different samples was much higher in the culture dish group than in the gelatin and gelatin–collagen scaffold groups. Moreover, the slopes of the earlier curves were calculated and the elastic moduli were acquired, which are presented in Table 1.

Since the deformation of the scaffold for culturing cells is very small, the elastic modulus of the small strain region

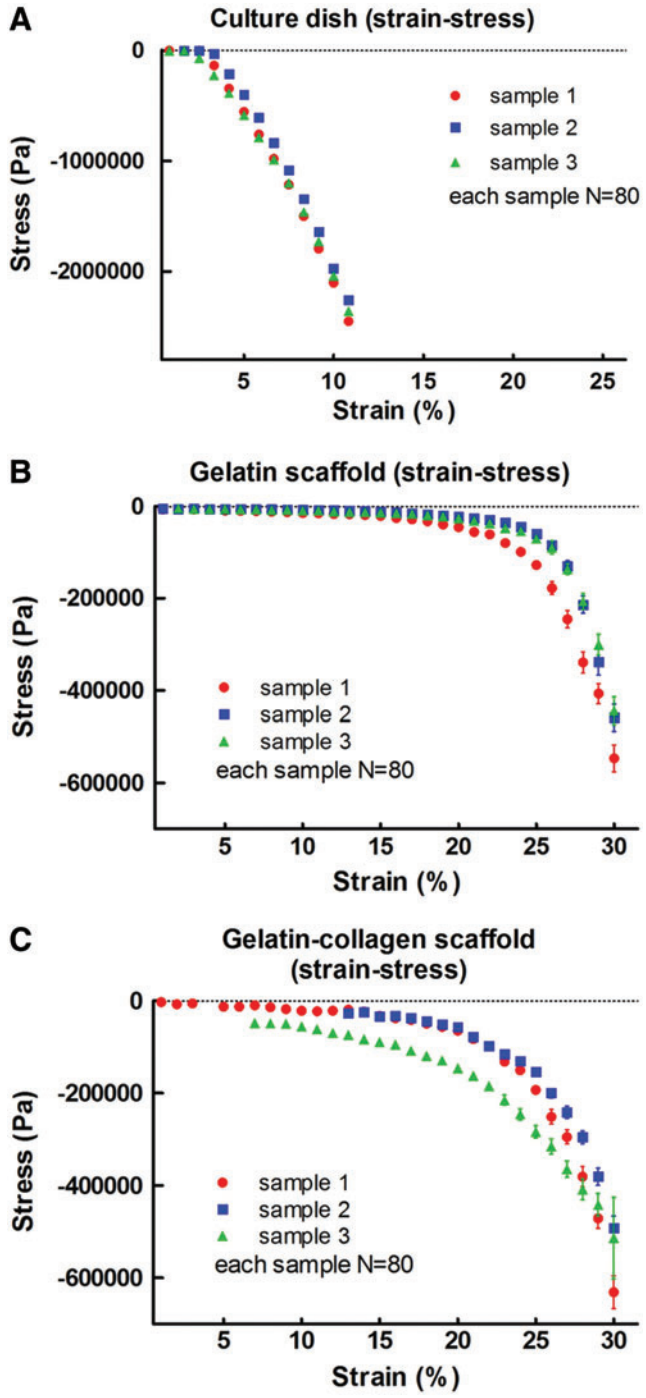

FIG. 5. The strain–stress curves (**A–C**) of the culture dish and 3D scaffold (gelatin, gelatin-collagen). The strain–stress curves of the culture dish, gelatin scaffold, and gelatin–collagen scaffold are shown in **A–C**, respectively. Moreover, the slopes of the above curves were calculated and the elastic moduli were acquired, which are presented in Table 1. N: times of measurements ($N = 80$), and 1–3 presents the encoded sample number. Color images available online at www.liebertpub.com/tea

(< 10%) was averaged. By this method, the elastic moduli (strain < 10%) of the culture dish, gelatin scaffold, and gelatin–collagen scaffold were about 28 Mpa, 60 kPa, and 220 kPa, respectively. Overall, the gelatin–collagen scaffold was harder than the gelatin scaffold.

TABLE 1. THE ELASTIC MODULUS OF CULTURE DISH, GELATIN SCAFFOLD, AND GELATIN–COLLAGEN SCAFFOLD, AND SPONTANEOUS CONTRACTION DAYS OF CARDIOMYOCYTES CULTURED IN THE ABOVE MATERIALS

	Culture dish	*Gelatin scaffold*	*Gelatin–collagen scaffold*
Elastic modulus	~28 MPa	~60 kPa	~220 kPa
Contraction days	13 days	25 days	19 days

Fluorescence staining

For the *in vitro* culture of cardiomyocytes, cells were required to get used to the new environment, such as a polystyrene culture plate. Since the environment is different from the original natural environment, the cells may change their behavior. One of the methods to evaluate cell health condition was fluorescence staining. Figure 6A shows the cardiomyocytes cultured on a 2D culture dish for 2 days and stained with anti-α-actinin antibody, anti-mouse IgG (whole molecule)-FITC, and DAPI. Through this procedure, the alignment of α-actinin and the position of nuclei were obtained. After cardiomyocytes were harvested for 2 days, the cells were getting used to the new environment. There was annular α-actinin around the nucleus (Fig. 6A), different from the morphology *in vivo* (striated α-actinin).[47] In other words, α-actinin was concentrated near the nucleus. When cardiomyocytes were cultured in a 2D environment for 6 days, the cytoskeleton, including f-actin (red) and α-actinin (green), spread out (Fig. 6B). The *in vivo* morphology of cardiomyocytes did not seem to appear after 6 days of culturing.

Figure 7 shows the 3D culture of cardiomyocytes using gelatin scaffolds. The green region represents the α-actinin. The merged images (lower column) were composed of the bright field that revealed the bubble position, the green region which represented the α-actini, and the blue region which pointed out the nuclei. According to the images, the striated α-actinin did not appear after harvesting for 2 days, but appeared on the fourth day after harvesting. Even until the eighth day, α-actinin remained in striated form, which meant that cardiomyocytes can stay healthy in this kind of 3D microenvironment.

Comparing the α-actinin morphologies of cardiomyocytes of 2D and 3D culture (Figs. 6 and 7), the striated α-actinin appeared only in the 3D gelatin scaffold. According to previous studies, cardiomyocytes on 10 kPa substrates developed aligned sarcomeres, whereas cells on stiffer substrates had unaligned sarcomeres and stress fibers, which are not observed *in vivo*.[47] It was found that cells generated greater mechanical force on gels with stiffnesses similar to that of the native myocardium, 10 kPa, than on stiffer or softer substrates. In other words, the best condition of stiffness for cardiomyocyte culture *in vitro* is about 10 kPa. Furthermore, in the 3D gelatin scaffold, compared with the 2D culture dish and 3D gelatin–collagen scaffold, the stiffness was more proximal to that of the native myocardium. Therefore, the clearest striated α-actinin appeared in the 3D gelatin scaffold (Fig. 7), but not in the 3D gelatin–collagen scaffold and 2D culture dish. As a result, the 3D gelatin scaffold is more suitable for cardiomyocyte culture than the 3D gelatin–collagen scaffold, due to the stiffnesses of the two scaffolds and the cytoskeleton distributions.

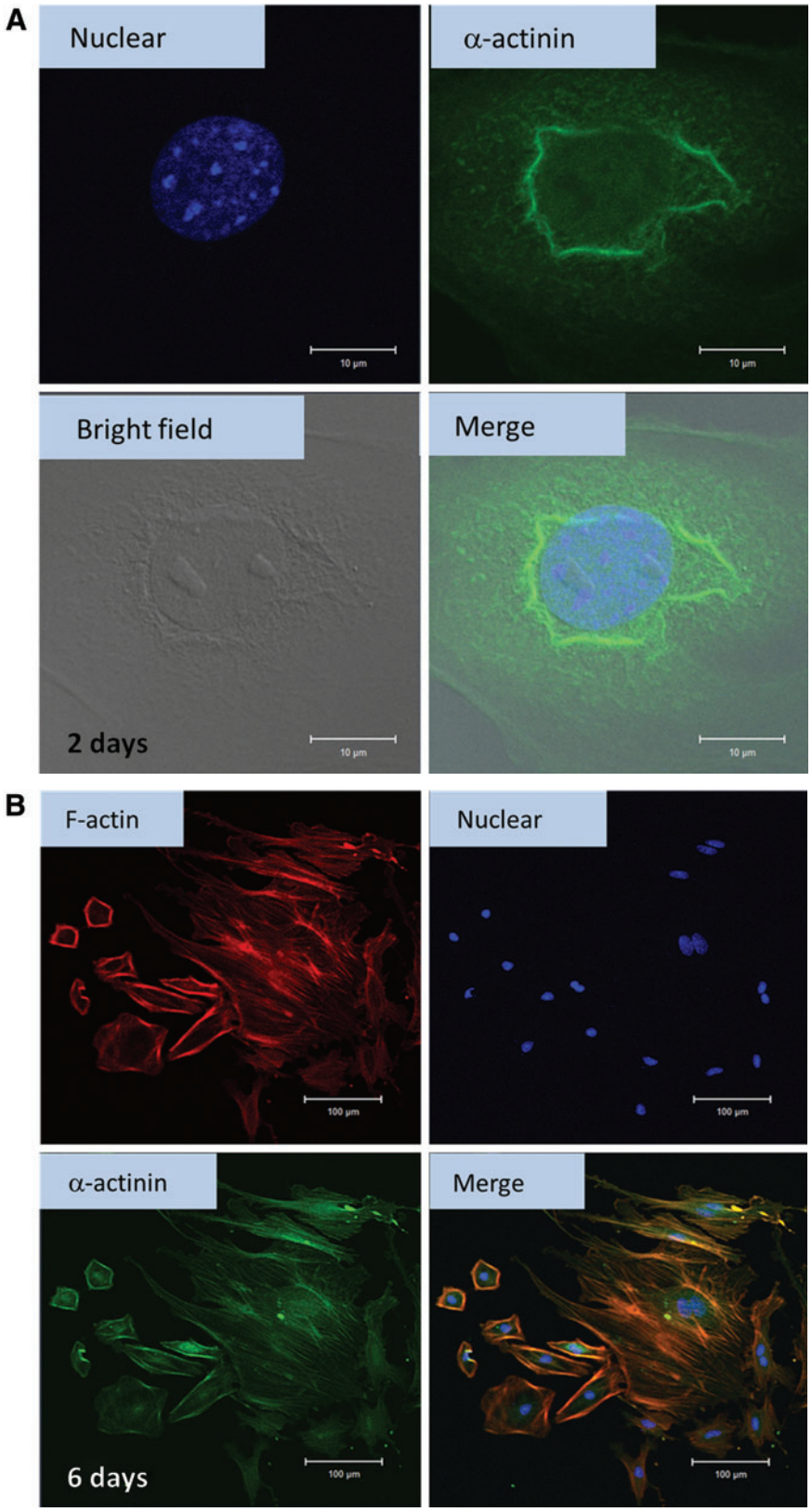

FIG. 6. **(A)** Cardiomyocytes cultured in two-dimensional (2D) cultured dish (for 2 days) and stained with anti-α-actinin, anti-mouse IgG (whole molecule)-FITC, and DAPI. In each figure, the images of nuclear, α-actinin, bright field, and the merging of the above three images of cardiomyocytes are presented. **(B)** Cardiomyocytes cultured in 2D cultured dish (for 6 days) and stained with anti-α-actinin, anti-mouse IgG (whole molecule)-FITC, DAPI, and phalloidin. In each figure, the images of f-actin, nuclear, α-actinin, and the merging of the above three images of cardiomyocytes are presented. Color images available online at www.liebertpub.com/tea

Cardiomyocytes cultured on 2D environment

After cardiomyocytes were seeded on a 2D culture dish for 1 day, some of the cells started beating. When cardiomyocytes were isolated from embryos and grown *in vitro*, they attached to an artificial substrate, and their beating rates decreased with culturing time. After about 2 weeks since the cardiomyocytes were harvested, the cells had lost their beating ability little by little, and it was hard to find any beating cells on the 2D culture dish. Cardiomyocytes tended

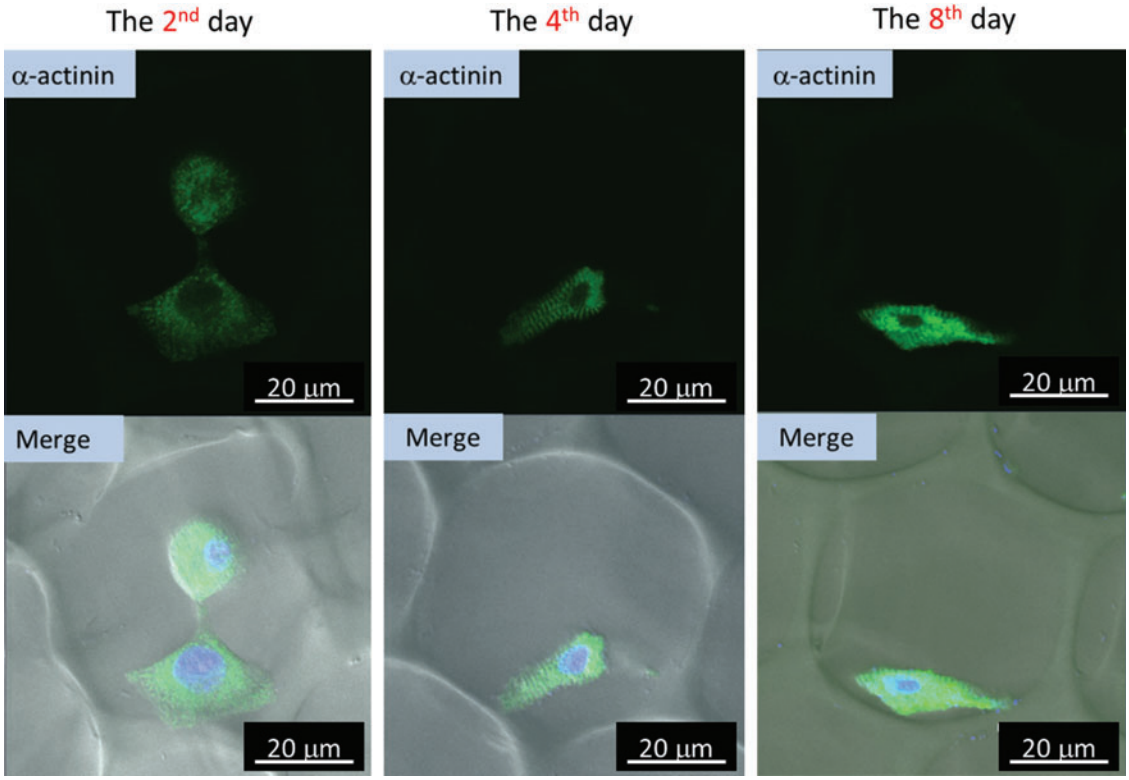

FIG. 7. Cardiomyocytes cultured in 3D gelatin scaffold (for 2, 4, and 8 days) and stained with anti-α-actinin, anti-mouse IgG (whole molecule)-FITC, and DAPI. The left column was the 2nd day culture, the middle column was the 4th day culture, and the right column was the 8th day culture. In the upper column, the green region indicates the position of α-actinin. In the lower column, which contains the merged images, the green region indicates the position of α-actinin, and the blue region represents the position of the nucleus; the bubble structure can be seen in the figure. Color images available online at www.liebertpub.com/tea

to aggregate if they were very close, and once they contacted each other for some time, they began beating in synchronization. As Figure 8A shows, in the red box, there were four cardiomyocytes beating synchronously. Actually, the procedure that was used to harvest cardiomyocytes could not separate cardiomyocytes and cardiac fibroblasts, but, at most, could raise the fraction of cardiomyocytes to cardiac fibroblasts through a preplating step; so there were still some cardiac fibroblasts which could not beat spontaneously. However, the cells were able to form a cell sheet containing cardiomyocytes and cardiac fibroblasts, if the cell density was high enough. When this condition was reached, the cardiomyocytes would drag cardiac fibroblasts along into beating together, as shown in Figure 8B. The existence of cardiac fibroblasts was important for creating a cardiac cell sheet,[45] so we cannot exclude all the cardiac fibroblasts.

Cardiomyocytes cultured in a 3D environment

Similar to the 2D culture, cardiomyocytes cultured in the 3D environment began beating at 2 days after harvesting, after acclimating to the *in vitro* environment. The beating frequency also decreased with an increase in culturing days. Figure 8C–H indicates that cardiomyocytes beat on different culturing days after isolation, and the red boxes point out the beating cell sites. As in 2D culture, if the cell density is high enough, cardiomyocytes and cardiac fibroblasts can connect with each other and form a cell sheet. Thus, the entire scaffold can contract through 3D cardiomyocyte sheets as well. Cardiomyocytes can, therefore, be cultured in both 3D gelatin and collagen-doped gelatin scaffolds.

The images of cardiomyocytes cultured in 3D gelatin scaffolds on different culturing days are shown in Figure 8C and D, and the beating behaviors were recorded in Supplementary Videos (Supplementary Data are available online at www.liebertpub.com/tea). The most obvious beating behavior can be observed in videos (Fig. 8C, day 11), and under this view, the entire scaffold was contracted by the beating cardiomyocytes. As the culturing days increased, fewer beating cardiomyocytes could be found, and the scaffold was partially reorganized by the cardiomyocytes. From Supplementary Videos, asynchronous contraction occurred in Figure 8D, in the red box. The last day we observed beating cardiomyocytes was 25 days after harvesting.

On the other hand, the images of cardiomyocytes cultured in the 3D gelatin–collagen scaffolds on different culturing days are shown in Figure 8E to H, and the beating behaviors were recorded in Supplementary Videos. As discussed earlier, interconnecting pores appeared during the degassing step, enabling cells in the scaffold to connect with each other. There is proof that the cardiomyocytes linked with each other and shared the same contraction frequency in the video. According to video, Figure 8F, cardiomyocytes in the entire view

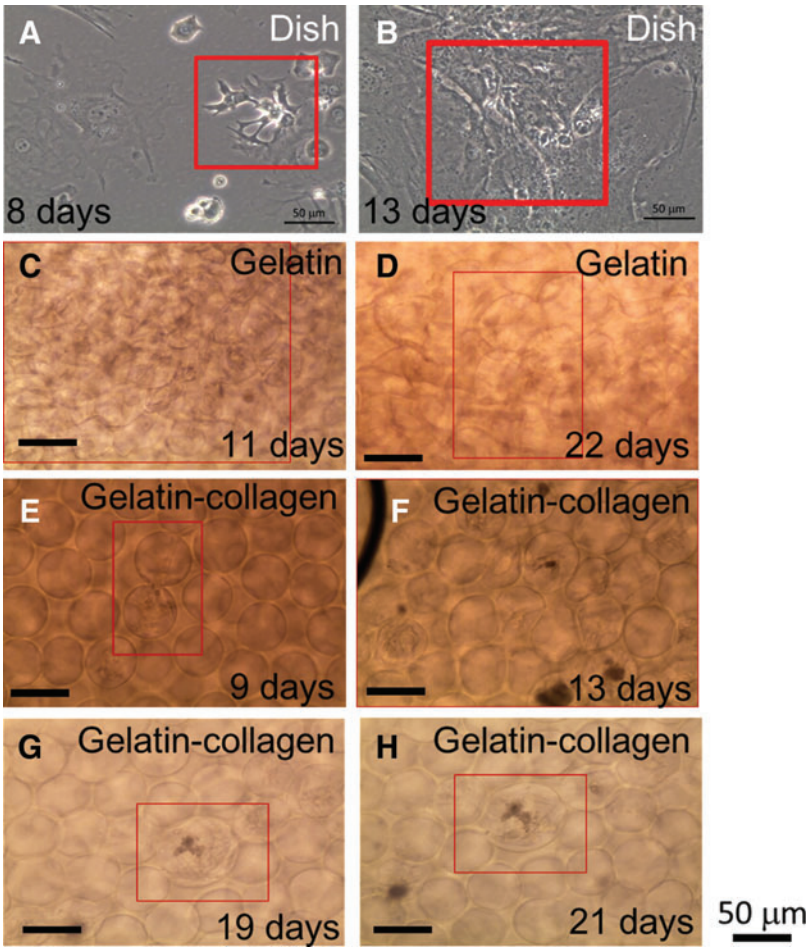

FIG. 8. **(A, B)** Morphology of cardiomyocytes on 2D culture dish. **(A)** Day 8, four cardiomyocytes in proximity were contracting in synchrony. **(B)** Day 13, an entire cellular sheet composed of cardiomyocytes and cardiac fibroblasts. **(C, D)** Cardiomyocytes cultured in 3D gelatin scaffold on different culturing days, **(C)** 11 days, **(D)** 22 days. **(E–H)** Cardiomyocytes cultured in 3D gelatin–collagen scaffold on different culturing days, **(E)** 9 days, **(F)** 13 days, **(G)** 19 days, and **(H)** 21 days. The red box in each figure indicates the beating region of the cardiomyocytes. There were Supplementary Videos to record the beating behavior of cardiomyocytes. The days of displaying spontaneous contraction of cardiomyocytes cultured in a 3D gelatin scaffold, 3D gelatin–collagen scaffold, and 2D culture dish are presented in Table 1. Color images available online at www.liebertpub.com/tea

contracted at a steady rate, and the scaffolds were contracted by the cardiomyocytes as well. Compared with other videos (Fig. 8G, H), the same cardiomyocytes beat at the 19th day but stop beating at the 21st day after harvesting.

Contraction of cardiomyocytes cultured in different materials

The spontaneous contraction days of cardiomyocytes cultured in 3D gelatin scaffold, 3D gelatin–collagen scaffold, and 2D culture dish were recorded and analyzed in Table 1. As a control group, primary culture cardiomyocytes seeded in a 2D culture dish were able to retain their contraction ability after harvesting from mice for only 13 days. Furthermore, cardiomyocytes cultured on this plastic material died about 2 weeks after they lost their natural growth environment. When cardiomyocytes were cultured in a 3D gelatin scaffold, the beating behavior was prolonged to 25 days, 12 days longer than when cultured in a biocompatible but man-made microenvironment. In other words, this platform can provide better conditions to sustain cardiomyocyte contraction behavior than traditional 2D culture dishes, nearly double the contraction time compared with that for 2D culture. However, beating cardiomyocytes were found till the 19th day of culturing in the 3D gelatin–collagen scaffold. To sum up, in culturing cardiomyocytes, the 3D gelatin scaffold was better than the 3D gelatin–collagen scaffold for sustaining contraction behavior, and both these materials were more suitable than a 2D traditional culture.

As previously mentioned in the introduction section, the beating frequency is an indication of the health condition of cardiomyocytes.[46] Here, we found that after cardiomyocytes were harvested from mice, the cells seeded in a 2D traditional culture dish died after about 2 weeks of culturing, which was shorter than for other culturing groups. We hypothesized several reasons for this phenomenon. First, a 2D microenvironment, which is far from a natural environment (3D), could not mimic the *in vivo* microenvironment of the cell under *in vitro* conditions. Second, the main material of dish was plastic, which is not biocompatible or biodegradable. In other words, plastic is not a natural material, but an artificial substrate. Third, if the substrate stiffness is hypothesized to affect cardiomyocyte activity, the culture dish, whose stiffness was about 28 MPa, was much stiffer than the native myocardium ($\sim$10 kPa).[47] The cultured cardiomyocytes were not accustomed to the material to which they attached; therefore, the cells died sooner on the plastic dish than on other substrates (Supplementary Figs. S1–S4).

Although the gelatin scaffold and gelatin–collagen scaffold provided a 3D micro environment for cardiomyocyte culture, there were still some differences between the two types of scaffolds. According to our results, gelatin seems more suitable for cardiomyocyte culture than collagen blended with gelatin. However, this seems to contradict the

observation, because collagen is more natural than gelatin and gelatin is denatured collagen. Referring to the mechanical properties, the elastic modulus of the 3D gelatin scaffold was about 60 kPa, and the 3D gelatin–collagen scaffold had an elastic modulus of about 220 kPa. On comparing these two materials, we see that the gelatin scaffold is closer in stiffness than the gelatin–collagen scaffold to the native myocardium, which has a stiffness of 10 kPa. This difference provides a possible reason that cardiomyocytes retained their contraction ability longer in the 3D gelatin scaffold (25 days) than in the 3D collagen-gelatin scaffold (19 days). As a result, we can apply this microfluidic technique to make 3D scaffolds for hosting healthy cardiomyocytes (maybe differentiated from stem cells) and choose gelatin as the main material for curing heart disease in the near future.

The advantages and challenges of these 3D cell culture scaffolds

Many studies have recently been published about cell behavior in 3D environments. Three-dimensional cell cultures mimic the natural tissue environment; on the other hand, 2D culture dishes or flasks are made of plastic, which is much harder than the natural tissue environment. Furthermore, close interactions between cells, ECMs, and growth factors in a 3D culture system can be achieved, while the cell–cell interaction on 2D culture dishes is little. Although nutrient diffusion is rapid on 2D culture dishes, cell–cell communication is regulated by biochemical gradients in a 3D culture, which is still more physiological than a 2D culture.

For this kind of 3D culture system, the process of making scaffolds was easily operated, because the scaffolds were made by microfluidic techniques. This strategy also saves time and money; it took about 1 min to fabricate one scaffold, and each scaffold cost less than 1 dollar. Depending on the cell size, we can tune the bubble diameter by adjusting air pressure and liquid flow rate, to optimize the cell culture conditions. Furthermore, we can change the liquid composition to influence the mechanical properties of the scaffold. For example, the osteocytes require harder substrates, in contrast to neurons, which prefer softer substrates. When the cells were seeded in the porous scaffolds, they were able to connect with each other through the interconnecting pores that formed in the degassing step. Due to limitations in imaging techniques, the 3D cell images were not as clear as the 2D cell images. For instance, cellular actin filaments could not be distinguished clearly in the 3D images.

Conclusions

In this work, 3D cell culture scaffolds were produced by microfluidic techniques, and the 3D scaffolds had better practicability, such as size tunability than traditional 2D culture dishes, as demonstrated by a series of experiments. Primary culture cardiomyocytes were seeded into the 3D scaffolds, composed of gelatin and collagen. A stiffness test of the scaffolds showed that the gelatin scaffold had more suitable mechanical properties for cardiomyocyte culture than the gelatin–collagen scaffold. The staining results also showed that cardiomyocytes can retain *in vivo* morphologies in the gelatin scaffold. Furthermore, cardiomyocytes can maintain their spontaneous contraction behavior *in vitro* for more days (25 days) in the gelatin scaffold than in the gelatin–collagen scaffold (19 days) and control culture dish (13 days). We believe that understanding cardiomyocyte behavior in a 3D environment will increase the probability of succeeding in myocardial tissue engineering and even repairing an injured heart.

Disclosure Statement

No competing financial interests exist.

References

1. Matsuura, K., Honda, A., Nagai, T., Fukushima, N., Iwanaga, K., Tokunaga, M., *et al.* Transplantation of cardiac progenitor cells ameliorates cardiac dysfunction after myocardial infarction in mice. J Clin Invest **119,** 2204, 2009.
2. Shah, U., Bien, H., and Entcheva, E. Microtopographical effects of natural scaffolding on cardiomyocyte function and arrhythmogenesis. Acta Biomater **6,** 3029, 2010.
3. Giraud, M.N., Armbruster, C., Carrel, T., and Tevaearai, H.T. Current state of the art in myocardial tissue engineering. Tissue Eng **13,** 1825, 2007.
4. Zimmermann, W.H., Didie, M., Doker, S., Melnychenko, I., Naito, H., Rogge, C., *et al.* Heart muscle engineering: an update on cardiac muscle replacement therapy. Cardiovasc Res **71,** 419, 2006.
5. Czubryt, M.P. Common threads in cardiac fibrosis, infarct scar formation, and wound healing. Fibrogenesis Tissue Repair **5,** 19, 2012.
6. Stout, D.A., Basu, B., and Webster, T.J. Poly(lactic–co-glycolic acid): carbon nanofiber composites for myocardial tissue engineering applications. Acta Biomater **7,** 3101, 2011.
7. Mironov, V., Boland, T., Trusk, T., Forgacs, G., and Markwald, R.R. Organ printing: computer-aided jet-based 3D tissue engineering. Trends Biotechnol **21,** 157, 2003.
8. Cui, X., and Boland, T. Human microvasculature fabrication using thermal inkjet printing technology. Biomaterials **30,** 6221, 2009.
9. Liao, Y.-C., Ma, Y.-T., Huang, C.-H., Yu, J., and Hsiao, H.-M. Rigidity guided cell attachment on inkjet-printed patterns. ACS Appl Mater Interfaces **4,** 3335, 2012.
10. Ramaswamy, S., Gottlieb, D., Engelmayr, G.C., Aikawa, E., Schmidt, D.E., Gaitan-Leon, D.M., *et al.* The role of organ level conditioning on the promotion of engineered heart valve tissue development *in-vitro* using mesenchymal stem cells. Biomaterials **31,** 1114, 2010.
11. Chen, C.-H., Chang, Y., Wang, C.-C., Huang, C.-H., Huang, C.-C., Yeh, Y.-C., *et al.* Construction and characterization of fragmented mesenchymal-stem-cell sheets for intramuscular injection. Biomaterials **28,** 4643, 2007.
12. Shintani, Y., Fukushima, S., Varela-Carver, A., Lee, J., Coppen, S.R., Takahashi, K., *et al.* Donor cell-type specific paracrine effects of cell transplantation for post-infarction heart failure. J Mol Cell Cardiol **47,** 288, 2009.
13. Callegari, A., Bollini, S., Iop, L., Chiavegato, A., Torregrossa, G., Pozzobon, M., *et al.* Neovascularization induced by porous collagen scaffold implanted on intact and cryoinjured rat hearts. Biomaterials **28,** 5449, 2007.
14. Siepe, M., Giraud, M.-N., Pavlovic, M., Receputo, C., Beyersdorf, F., Menasché, P., *et al.* Myoblast-seeded biodegradable scaffolds to prevent post–myocardial infarction evolution toward heart failure. J Thorac Cardiovasc Surg **132,** 124, 2006.
15. Taylor, P.M., Cass, A.E.G., and Yacoub, M.H. Extracellular matrix scaffolds for tissue engineering heart valves. Prog Pediatr Cardiol **21,** 219, 2006.

16. Yeong, W.Y., Sudarmadji, N., Yu, H.Y., Chua, C.K., Leong, K.F., Venkatraman, S.S., *et al.* Porous polycaprolactone scaffold for cardiac tissue engineering fabricated by selective laser sintering. Acta Biomater **6,** 2028, 2010.
17. Xiang, Z., Liao, R.L., Kelly, M.S., and Spector, M. Collagen-GAG scaffolds grafted onto myocardial infarcts in a rat model: a delivery vehicle for mesenchymal stem cells. Tissue Eng **12,** 2467, 2006.
18. LaFramboise, W.A., Scalise, D., Stoodley, P., Graner, S.R., Guthrie, R.D., Magovern, J.A., *et al.* Cardiac fibroblasts influence cardiomyocyte phenotype *in vitro*. Am J Physiol Cell Physiol **292,** C1799, 2007.
19. Radisic, M., Park, H., Chen, F., Salazar-Lazzaro, J.E., Wang, Y.D., Dennis, R., *et al.* Biomirnetic approach to cardiac tissue engineering: oxygen carriers and channeled scaffolds. Tissue Eng **12,** 2077, 2006.
20. Sreejit, P., Kumar, S., and Verma, R.S. An improved protocol for primary culture of cardiomyocyte from neonatal mice. In Vitro Cell Dev Biolo Anim **44,** 45, 2008.
21. Nguyen, P.D., Hsiao, S.T., Sivakumaran, P., Lim, S.Y., and Dilley, R.J. Enrichment of neonatal rat cardiomyocytes in primary culture facilitates long-term maintenance of contractility *in vitro*. Am J Physiol Cell Physiol **303,** C1220, 2012.
22. Pego, A.P., Siebum, B., Van Luyn, M.J.A., Van Seijen, X., Poot, A.A., Grijpma, D.W., *et al.* Preparation of degradable porous structures based on 1,3-trimethylene carbonate and D,L-lactide (co)polymers for heart tissue engineering. Tissue Eng **9,** 981, 2003.
23. LaNasa, S.M., and Bryant, S.J. Influence of ECM proteins and their analogs on cells cultured on 2-D hydrogels for cardiac muscle tissue engineering. Acta Biomater **5,** 2929, 2009.
24. Pok, S., Myers, J.D., Madihally, S.V., and Jacot, J.G. A multilayered scaffold of a chitosan and gelatin hydrogel supported by a PCL core for cardiac tissue engineering. Acta Biomater **9,** 5630, 2013.
25. Smith, A.W., Segar, C.E., Nguyen, P.K., MacEwan, M.R., Efimov, I.R., and Elbert, D.L. Long-term culture of HL-1 cardiomyocytes in modular poly(ethylene glycol) microsphere-based scaffolds crosslinked in the phase-separated state. Acta Biomater **8,** 31, 2012.
26. Kubo, H., Shimizu, T., Yamato, M., Fujimoto, T., and Okano T. Creation of myocardial tubes using cardiomyocyte sheets and an *in vitro* cell sheet-wrapping device. Biomaterials **28,** 3508, 2007.
27. Haraguchi, Y., Shimizu, T., Yamato, M., Kikuchi, A., and Okano, T. Electrical coupling of cardiomyocyte sheets occurs rapidly via functional gap junction formation. Biomaterials **27,** 4765, 2006.
28. Shimizu, T., Sekine, H., Isoi, Y., Yamato, M., Kikuchi, A., and Okano, T. Long-term survival and growth of pulsatile myocardial tissue grafts engineered by the layering of cardiomyocyte sheets. Tissue Eng **12,** 499, 2006.
29. Wang, P.-Y., Yu, J., Lin, J.-H., and Tsai, W.-B. Modulation of alignment, elongation and contraction of cardiomyocytes through a combination of nanotopography and rigidity of substrates. Acta Biomater **7,** 3285, 2011.
30. Kelm, J.M., Ehler, E., Nielsen, L.K., Schlatter, S., Perriard, J.C., and Fussenegger, M. Design of artificial myocardial microtissues. Tissue Eng **10,** 201, 2004.
31. Yu, J.S., Du, K.T., Fang, Q.Z., Gu, Y.P., Mihardja, S.S., Sievers, R.E., *et al.* The use of human mesenchymal stem cells encapsulated in RGD modified alginate microspheres in the repair of myocardial infarction in the rat. Biomaterials **31,** 7012, 2010.
32. Faraj, K.A., Van Kuppevelt, T.H., and Daamen, W.F. Construction of collagen scaffolds that mimic the three-dimensional architecture of specific tissues. Tissue Eng **13,** 2387, 2007.
33. Shea, L.D., Wang, D., Franceschi, R.T., and Mooney, D.J. Engineered bone development from a pre-osteoblast cell line on three-dimensional scaffolds. Tissue Eng **6,** 605, 2000.
34. Botchwey, E.A., Pollack, S.R., Levine, E.M., and Laurencin, C.T. Bone tissue engineering in a rotating bioreactor using a microcarrier matrix system. J Biomed Mater Res **55,** 242, 2001.
35. Chiu, P.-J., Mei, J.-C., Huang, Y.-C., and Yu, J. Monolayer microbubbles fabricated by microfluidic device for keratocytes observation. Microelectron Eng **111,** 277, 2013.
36. Page, H., Flood, P., and Reynaud, E.G. Three-dimensional tissue cultures: current trends and beyond. Cell Tissue Res **352,** 123, 2013.
37. Griffith, L.G., and Swartz, M.A. Capturing complex 3D tissue physiology *in vitro*. Nat Rev Mol Cell Biol **7,** 211, 2006.
38. El-Ali, J., Sorger, P.K., and Jensen, K.F. Cells on chips. Nature **442,** 403, 2006.
39. Gillette, B.M., Jensen, J.A., Tang, B.X., Yang, G.J., Bazargan-Lari, A., Zhong, M., *et al. In situ* collagen assembly for integrating microfabricated three-dimensional cell-seeded matrices. Nat Mater **7,** 636, 2008.
40. Chung, K.Y., Mishra, N.C., Wang, C.C., Lin, F.H., and Lin, K.H. Fabricating scaffolds by microfluidics. Biomicrofluidics **3,** 022403, 2009.
41. Lin, J.-Y., Lin, W.-J., Hong, W.-H., Hung, W.-C., Nowotarski, S.H., Gouveia, S.M., *et al.* Morphology and organization of tissue cells in 3D microenvironment of monodisperse foam scaffolds. Soft Matter **7,** 10010, 2011.
42. Pego, A.P., Poot, A.A., Grijpma, D.W., and Feijen, J. Biodegradable elastomeric scaffolds for soft tissue engineering. J Control Release **87,** 69, 2003.
43. Radisic, M., and Vunjak-Novakovic, G. Cardiac tissue engineering. J Serb Chem Soc **70,** 541, 2005.
44. Hidalgobastida, L., Barry, J., Everitt, N., Rose, F., Buttery, L., Hall, I., *et al.* Cell adhesion and mechanical properties of a flexible scaffold for cardiac tissue engineering. Acta Biomater **3,** 457, 2007.
45. Matsuura, K., Masuda, S., Haraguchi, Y., Yasuda, N., Shimizu, T., Hagiwara, N., *et al.* Creation of mouse embryonic stem cell-derived cardiac cell sheets. Biomaterials **32,** 7355, 2011.
46. Janowska-Kulinska, A., Torzynska, K., Markiewicz-Grochowalska, A., Sowinska, A., Majewski, M., Jerzykowska, O., *et al.* Changes in heart rate variability caused by coronary angioplasty depend on the localisation of coronary lesions. Kardiol Pol **67,** 130, 2009.
47. Jacot, J.G., McCulloch, A.D., and Omens, J.H. Substrate stiffness affects the functional maturation of neonatal rat ventricular myocytes. Biophys J **95,** 3479, 2008.

Address correspondence to:
Jiashing Yu, PhD
Department of Chemical Engineering
National Taiwan University
No. 1, Roosevelt Rd., Sec. 4
Taipei 106
Taiwan

E-mail: jiayu@ntu.edu.tw

Received: September 3, 2013
Accepted: April 25, 2014
Online Publication Date: July 18, 2014